doi:10.3772/j.issn.1006-6748.2019.03.011

# Robust $H\infty$ output tracking control of uncertain networked control systems[①]

Liu Yicai (刘义才)[②] [*] [**], Liu Bin [*]

( [*] Engineering Research Center for Metallurgical Automation and Detecting Technology of Ministry of Education; Institute of Information Science and Engineering, Wuhan University of Science and Technology, Wuhan 430081, P. R. China)

( [**] School of Mechanical-electronic and Automobile Engineering, Wuhan Business University, Wuhan 430056, P. R. China)

**Abstract**

This paper investigates a problem of robust output tracking control of networked control systems (NCSs) with network-induced delays, packet dropouts, parameter uncertainties and external disturbances. Firstly, an augmented model of time-delay system is proposed for networked tracking control systems. Then, considering the piecewise differentiable characteristic of time-delay, the criterion to output tracking performance analysis and controller design are derived by using an approach of free weighting matrix, reciprocally convex and cone complementarity linearization (CCL). Finally, simulation results of numerical examples show the effectiveness of the proposed approach, and illustrate the advantages of the proposed criteria which outperform previous criteria in the literature.

**Key words**: networked control systems (NCSs), H∞ output tracking control, time-delay systems, cone complementarity linearization

## 0 Introduction

Compared with the traditional point to point control system, networked control systems (NCSs) can be potentially designed into large-scale systems and widely used in many fields due to its easy installation, maintenance, convenient layout and high flexibility. However, integration of communication networks into feedback control loops inevitably leads to non-ideal network quality of services, e.g., network-induced delays, data packet dropouts and disorder, which make the analysis and design of NCSs more complex than those for traditional control systems[1-3]. Therefore, enormous attentions have been paid to the issues of stability analysis and stabilization controller design[4-8]. In addition to the requirement of system stabilization, tracking control which is widely used in mechanical systems, robot control, flight control[9-12], etc, can make the output of the plant track a prescribed reference trajectory. But its feedback control signal will lead to an output error as a result of the communication constraints in NCSs. So it is more challengeable to achieve desired tracking performance, especially under the influence of system parameter uncertainties and external disturbances. Until now, the studies of networked tracking control can be divided into two broad categories. One is the predictive control, the other is the robust control. The representative of the former is the research in Refs[13-16]. In Ref. [13], a delay dependent tracking controller was designed for NCSs with Markov delays. However, only the network induced delay was considered, and the Markov transition matrices must be known in advance. In Refs[14,15], the problem of networked output tracking control was studied by using predictive control to compensate for network-induced delay and packet dropouts actively. But the effects of uncertain parameters and external disturbances were not investigated. In Ref. [16], the tracking error and the state variables were combined and optimized together to deal with the NCSs under random packet dropouts and uncertainties. But only the fixed short time-delay was considered. The typical research of the latter is in Refs[17-22], which discussed the networked tracking control problem in the $H\infty$ sense. Ref. [20] addressed observer-based $H\infty$ output tracking control for NCSs by using the particle swarm optimization technique with feasibility of the LMI-based stability criterion. In Refs[21,22], the closed-loop NCSs were modeled as finite subsystems by gridding approach, and the mode-dependent robust $H\infty$ output tracking controller is obtained by the stochastic and switching system method, respectively.

During the last decade, various methods were de-

① Supported by the National Natural Science Foundation of China (No. 61104027, 61573263) and the Scientific Research Project of Hubei Provincial Department of Education (No. B2017280).

② To whom correspondence should be addressed. E-mail: liuyicai027@wbu.edu.cn

Received on Aug. 23, 2018

veloped to derive less conservative stability condition for time-delay systems and NCSs by different Lyapunov-Krasovskii functions. Particularly, the employments of various techniques have been proposed such as free-weighting matrix[23,24], Wirtinger-based integral inequality[25], relaxed integral inequalities[26], reciprocally convex approach[27,28], and delay partitioning method[29,30]. For instance, in Ref. [31], a less conservative result was obtained by constructing a novel Lyapunov-Krasovskii functional to consider the interval delay information, and using the reciprocally convex approach.

Motivated by the above analysis, in this paper, robust $H\infty$ output tracking control is dealt with for the piecewise continuous-time-varying delay system. A state feedback controller is aimed to design to achieve output tracking performance for NCSs. It should be pointed out that the proposed method can be suitable for the NCSs stability problem and can also yield less conservative result. The main contributions of this paper can be identified as follows.

1) Compared with the predictive control method, the proposed method has investigated more general NCSs with network-induced time-varying delay, packet dropouts, parameter uncertainties and external disturbances.

2) The performance of output tracking control under investigation is transformed into the robust $H\infty$ control performance, and the less conservative criterion can be obtained by using new approach.

This paper is organized as follows. In Section 1, an augmented model of time-delay systems for networked output tracking control systems is proposed. Then $H\infty$ output tracking performance is analyzed in Section 2. Section 3 proposes a design method of $H\infty$ output tracking controller. Finally, the proposed method is illustrated by numerical examples in Section 4 which is followed by conclusions in Section 5.

**Notation** The notation used throughout the paper is fairly standard. $N$ stands for the set of positive integers. $\boldsymbol{R}^n$ denotes the $n$-dimensional Euclidean space. $\boldsymbol{X} > 0$ ($\boldsymbol{X} < 0$) is used to represent a positive (negative) definite matrix. $\|\cdot\|_2$ marks the Euclidean norm. The symbol '$*$' represents the symmetric term in a symmetric matrix. And $diag\{\cdots\}$ denotes the block-diagonal matrix.

## 1 Problem description and system modeling

Consider the typical NCSs as shown in Fig. 1, and suppose the physical plant is given by the following model:

$$\begin{cases} \dot{\boldsymbol{x}}_p(t) = (\boldsymbol{A}_p + \Delta\boldsymbol{A}_p)\boldsymbol{x}_p(t) + (\boldsymbol{B}_p + \Delta\boldsymbol{B}_p)\boldsymbol{u}(t) \\ \qquad\quad + \boldsymbol{B}_\omega\boldsymbol{\omega}(t) \\ \boldsymbol{y}_p(t) = (\boldsymbol{C}_p + \Delta\boldsymbol{C}_p)\boldsymbol{x}_p(t) + (\boldsymbol{D}_p + \Delta\boldsymbol{D}_p)\boldsymbol{u}(t) \end{cases} \tag{1}$$

here, $\boldsymbol{x}(t) \in \boldsymbol{R}^n$, $\boldsymbol{u}(t) \in \boldsymbol{R}^m$ are the system state vector and the control input vector, respectively; $\boldsymbol{y}_p(t) \in \boldsymbol{R}^q$ is the output, and $\boldsymbol{\omega}(t) \in L_2[0, \infty)$ is the disturbance input; $\boldsymbol{A}_p$, $\boldsymbol{B}_p$, $\boldsymbol{C}_p$, $\boldsymbol{D}_p$ and $\boldsymbol{B}_\omega$ are constant matrices. $\Delta\boldsymbol{A}_p$, $\Delta\boldsymbol{B}_p$, $\Delta\boldsymbol{C}_p$ and $\Delta\boldsymbol{D}_p$ denote the parameter uncertainties, satisfying $[\Delta\boldsymbol{A}_p \;\; \Delta\boldsymbol{B}_p] = \boldsymbol{G}_p\boldsymbol{F}_p(t)[\boldsymbol{E}_{pa} \;\; \boldsymbol{E}_{pb}]$ and $[\Delta\boldsymbol{C}_p \;\; \Delta\boldsymbol{D}_p] = \boldsymbol{N}_p\boldsymbol{\Delta}_p(t)[\boldsymbol{E}_{pc} \;\; \boldsymbol{E}_{pd}]$, where $\boldsymbol{F}_p(t)$, $\boldsymbol{\Delta}_p(t)$ are the unknown time-varying matrices, satisfying $\|\boldsymbol{F}_p^{\mathrm{T}}(t)\boldsymbol{F}_p(t)\|_2 < \boldsymbol{I}$ and $\|\boldsymbol{\Delta}_p^{\mathrm{T}}(t)\boldsymbol{\Delta}_p(t)\|_2 < \boldsymbol{I}$, $\forall t$.

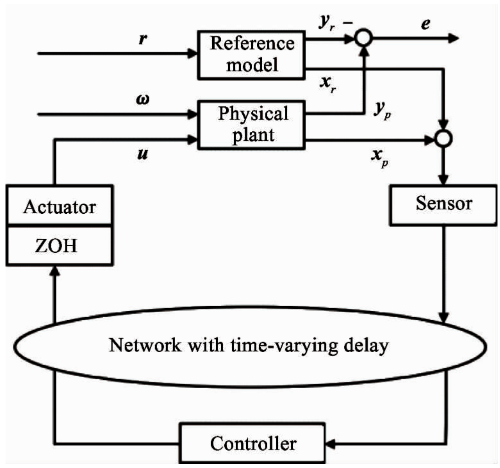


**Fig. 1** Networked tracking control systems

The goal of this paper is to design a controller, such that the output $\boldsymbol{y}_p(t)$ of the NCSs can track a reference signal to meet the required tracking performance. Suppose the reference signal $\boldsymbol{y}_r(t)$ is generated by

$$\begin{cases} \dot{\boldsymbol{x}}_r(t) = \boldsymbol{A}_r\boldsymbol{x}_r(t) + \boldsymbol{B}_r\boldsymbol{r}(t) \\ \boldsymbol{y}_r(t) = \boldsymbol{C}_r\boldsymbol{x}_r(t) \end{cases} \tag{2}$$

where $\boldsymbol{y}_r(t)$ has the same dimension as $\boldsymbol{y}(t)$; $\boldsymbol{x}_r(t)$, $\boldsymbol{r}(t) \in \boldsymbol{R}^r$ are reference state and energy bounded reference input, respectively; $\boldsymbol{A}_r$ and $\boldsymbol{C}_r$ are appropriately dimensioned constant matrices with $\boldsymbol{A}_r$ Hurwitz.

**Remark 1** Reference model Eq. (2) is the deterministic object designed artificially. It can determine every parameter of the model according to the need of input $\boldsymbol{r}(t)$ and output $\boldsymbol{y}_r(t)$, and usually require that the eigenvalue of the system matrix $\boldsymbol{A}_r$ is within the unit circle. Since physical plant Eq. (1) works in the actual environment, model parameter uncertainties, external input interference, and network environment with time delay and packet dropouts will have a negative impact on output, even cause the instability of the system. Therefore, it is desired to design a controller such that the plant's output $\boldsymbol{y}_p(t)$ to asymptotically track a given deterministic reference signal $\boldsymbol{y}_r(t)$.

Throughout this paper, it is assumed that system Eq. (1) is controlled through a network where network-induced delays and packet dropouts exist in both sensor-to-controller and controller-to-actuator channel as shown in Fig. 1. Before further proceeding, the following assumptions are given, which are common in NCSs research in the literature.

**Assumption 1** $h$ is the system constant sampling period and $i_k h$, $i_k \in N$ is sampling instant. The data is transmitted with a single-packet, and the out-of-sequence packet is discarded for the NCSs when a packet disordering occurs.

**Assumption 2** The ZOH (zero-order-hold) before the actuator is used to hold the actuator input value when there is no latest control packet arrived at the actuator.

**Assumption 3** Define $\tau_{t_k} = \tau_{t_k}^{sc} + \tau_{t_k}^{ca}$, where $\tau_{t_k}^{sc}$ and $\tau_{t_k}^{ca}$ represent network-induced time-varying delays which exist in sensor-to-controller and controller-to-actuator channel, respectively. In addition, the maximum number $d$ of consecutive packet dropouts in NCSs has an upper bound $\bar{d}$.

Considering the network-induced time-varying delays and packet dropouts which exist in sensor-to-controller and controller-to-actuator channels, the holding interval of the ZOH is $[\, i_k h + \tau_k \quad i_k h + (d+1)h + \tau_{k+1})$. By defining $\tau(t) = t - i_k h$, $\tau_1 = \tau_m \leqslant \tau(t) \leqslant (\bar{d}+1)h + \tau_M = \tau_2$ can be obtained, where $\tau_M$ and $\tau_m$ represent maximum and minimum network-induced time-varying delay, respectively. From the definition $\tau(t)$, $\tau(t)$ is piecewise-linear with the first derivative satisfying $\dot{\tau}(t) = 1$, but its first derivative does not exist at the sampling instant. Thus, in this paper, this characteristic is taken into consideration to reduce the analysis and design conservativeness.

Considering the behavior of ZOH, the state feedback control law can be expressed as

$$\begin{aligned}\boldsymbol{u}(t) &= \boldsymbol{K}_1\boldsymbol{x}_p(i_k h) + \boldsymbol{K}_2\boldsymbol{x}_r(i_k h)\\ &= \boldsymbol{K}_1\boldsymbol{x}_p(t-\tau(t)) + \boldsymbol{K}_2\boldsymbol{x}_r(t-\tau(t))\end{aligned} \tag{3}$$

where $K_1$ and $K_2$ are the state-feedback control gains to be determined. Therefore, the augmented closed-loop system can be obtained from Eqs(1) – (3) as follows.

$$\begin{cases}\boldsymbol{x}(t) = \bar{\boldsymbol{A}}x(t) + \bar{\boldsymbol{B}}\boldsymbol{K}\boldsymbol{x}(t-\tau(t)) + \bar{\boldsymbol{B}}_{\varpi}\boldsymbol{\varpi}(t)\\ \boldsymbol{e}(t) = \bar{\boldsymbol{C}}x(t) + \bar{\boldsymbol{D}}\boldsymbol{K}\boldsymbol{x}(t-\tau(t))\end{cases} \tag{4}$$

where $\boldsymbol{e}(t) = \boldsymbol{y}_p(t) - \boldsymbol{y}_r(t)$, $\boldsymbol{x}(t) = \begin{bmatrix}\boldsymbol{x}_p(t)\\ \boldsymbol{x}_r(t)\end{bmatrix}$, $\boldsymbol{\varpi}(t) = \begin{bmatrix}\boldsymbol{\omega}(t)\\ \boldsymbol{r}(t)\end{bmatrix}$, $\boldsymbol{K} = [\,\boldsymbol{K}_1 \quad \boldsymbol{K}_2\,]$, $\bar{\boldsymbol{A}} = \boldsymbol{A} + \boldsymbol{G}\boldsymbol{F}_p(t)\boldsymbol{E}_a$, $\bar{\boldsymbol{B}} = \boldsymbol{B} + \boldsymbol{G}\boldsymbol{F}_p(t)\boldsymbol{E}_b$, $\bar{\boldsymbol{B}}_{\varpi} = \begin{bmatrix}\boldsymbol{B}_{\omega} & 0\\ 0 & \boldsymbol{I}\end{bmatrix}$, $\boldsymbol{A} = \begin{bmatrix}\boldsymbol{A}_p & 0\\ 0 & \boldsymbol{A}_r\end{bmatrix}$, $\boldsymbol{B} = \begin{bmatrix}\boldsymbol{B}_p\\ 0\end{bmatrix}$, $\boldsymbol{G} = \begin{bmatrix}\boldsymbol{G}_p & 0\\ 0 & 0\end{bmatrix}$, $\boldsymbol{E}_a = \begin{bmatrix}\boldsymbol{E}_{pa} & 0\\ 0 & 0\end{bmatrix}$, $\boldsymbol{E}_b = \begin{bmatrix}\boldsymbol{E}_{pb}\\ 0\end{bmatrix}$, $\bar{\boldsymbol{C}} = \boldsymbol{C} + \boldsymbol{N}\boldsymbol{\Delta}_p(t)\boldsymbol{E}_c$, $\boldsymbol{D} = \boldsymbol{D}_p$, $\boldsymbol{C} = [\,\boldsymbol{C}_p \quad -\boldsymbol{C}_r\,]$, $\bar{\boldsymbol{D}} = \boldsymbol{D} + \boldsymbol{N}\boldsymbol{\Delta}_p(t)\boldsymbol{E}_d$, $\boldsymbol{N} = [\,\boldsymbol{N}_p \quad 0\,]$, $\boldsymbol{E}_c = \boldsymbol{E}_{pc}$, $\boldsymbol{E}_d = \begin{bmatrix}\boldsymbol{E}_{pd}\\ 0\end{bmatrix}$.

Then, the requirements of the $H\infty$ output tracking performance are presented as follows.

1) The augmented closed-loop system Eq. (4) with $\boldsymbol{\varpi}(t) = 0$ is asymptotically stable;

2) The effect of $\boldsymbol{\varpi}(t)$ on the tracking error $\boldsymbol{e}(t)$ is attenuated below a desired $H\infty$ performance. More specifically, it is required that $\|\boldsymbol{e}(t)\|_2 \leqslant \gamma \|\boldsymbol{\varpi}(t)\|_2$, where $\gamma > 0$.

**Remark 2** Network-induced delays, packet dropouts and variable sampling intervals are all taken into consideration by the time-varying input delay $\tau(t)$, and $\boldsymbol{\varpi}(t) = [\,\boldsymbol{\omega}^{\mathrm{T}}(t) \quad \boldsymbol{r}^{\mathrm{T}}(t)\,]^{\mathrm{T}}$ is regarded as the external input interference of the system Eq. (4) by the augmented model approach. Therefore, the problem of the actual physical plant Eq. (1) output $\boldsymbol{y}_p(t)$ tracking reference model Eq. (2) output $\boldsymbol{y}_r(t)$ is transformed into the robust control problem of the time-delay system. The purpose of this paper is therefore to design a robust state-feedback controller such that the output tracking performance is ensured in the $H\infty$ sense.

## 2 H∞ output tracking performance analysis

This section investigates the problem of $H\infty$ output tracking performance analysis. More specifically, assuming that the controller gain $\boldsymbol{K}$ is known, Theorem 1 proposes the conditions under which the augmented closed-loop system Eq. (4) can be asymptotically stable and achieve $H\infty$ output tracking performance $\gamma$. This Theorem is instrumental in the controller design problem. Firstly, some lemmas are given as below.

**Lemma 1** (Jensen's inequality[32]): For any constant matrix $\boldsymbol{S} \in \Re^n$, $\boldsymbol{S} = \boldsymbol{S}^{\mathrm{T}} > 0$, scalar $\sigma > 0$, and vector function $\dot{\boldsymbol{x}}(t): [-\sigma, \ 0] \rightarrow \Re^n$, such that the following integration is well defined, then

$$-\sigma\int_{-\sigma}^{0}\dot{\boldsymbol{x}}(t+v)\boldsymbol{S}\dot{\boldsymbol{x}}(t+v)\mathrm{d}v \leqslant \begin{bmatrix}\boldsymbol{x}(t)\\ \boldsymbol{x}(t-\sigma)\end{bmatrix}^{\mathrm{T}}\begin{bmatrix}-\boldsymbol{S} & *\\ \boldsymbol{S} & -\boldsymbol{S}\end{bmatrix}\begin{bmatrix}\boldsymbol{x}(t)\\ \boldsymbol{x}(t-\sigma)\end{bmatrix}$$

**Lemma 2** (Reciprocally convex approach[27]): Let $f_1, f_2, \cdots, f_N: R^m \rightarrow R$ have positive values in an open subset $D$ of $R^m$. Then, the reciprocally convex combination of $f_i$ over $D$ satisfies:

$$\min_{\{\beta_i | \beta_i > 0, \sum_i \beta_i = 1\}} \sum_i \frac{1}{\beta_i} f_i(t) = \sum_i f_i(t) + \max_{g_{i,j}} \sum_{i \neq j} g_{i,j}(t)$$

subject to

$$\left\{ g_{i,j}: \left( \Re^m \rightarrow \Re,\ g_{i,j}(t) = g_{j,i}(t), \begin{bmatrix} f_i(t) & g_{j,i}(t) \\ g_{i,j}(t) & f_j(t) \end{bmatrix} \geqslant 0 \right) \right\}$$

**Lemma 3**[33] $\boldsymbol{\Xi}_i (i = 1,2)$ and $\boldsymbol{\Omega}$ are matrices with appropriate dimensions, $\eta(t)$ is a function of $t$ and $\eta_1 \leqslant \eta(t) \leqslant \eta_2$, then $\eta(t)\boldsymbol{\Xi}_1 + (\eta_2 - \eta(t))\boldsymbol{\Xi}_2 + \boldsymbol{\Omega} < 0$ if and only if $\eta_1 \boldsymbol{\Xi}_1 + (\eta_2 - \eta_1)\boldsymbol{\Xi}_2 + \boldsymbol{\Omega} \leqslant 0$ and $\eta_2 \boldsymbol{\Xi}_1 + \boldsymbol{\Omega} < 0$.

**Theorem 1** For given scalars $\gamma$, $\tau_1$, $\tau_2$ and matrix $\boldsymbol{K}$, the augmented closed-loop system Eq. (4) is asymptotically stable and can achieve the $H\infty$ output tracking performance $\gamma$ if there exist matrices $\boldsymbol{X} > 0$, $\boldsymbol{Y} > 0$, $\boldsymbol{Q}_1 > 0$, $\boldsymbol{Q}_2 > 0$, $\boldsymbol{R}_1 > 0$, $\boldsymbol{R}_2 > 0$, $\boldsymbol{H} > 0$, $\boldsymbol{M}$ and $\boldsymbol{U}$ with appropriate dimensions such that:

$$\begin{bmatrix} \boldsymbol{R}_2 & * \\ \boldsymbol{U} & \boldsymbol{R}_2 \end{bmatrix} > 0 \tag{5}$$

$$\boldsymbol{\Xi}_1 = \begin{pmatrix} \boldsymbol{\Xi} + \tau_1 \boldsymbol{M}\boldsymbol{H}^{-1}\boldsymbol{M}^{\mathrm{T}} + \boldsymbol{M}(\boldsymbol{e}_1 - \boldsymbol{e}_3) \\ + (\boldsymbol{e}_1 - \boldsymbol{e}_3)^{\mathrm{T}}\boldsymbol{M}^{\mathrm{T}} + (\tau_2 - \tau_1)\boldsymbol{\Gamma}^{\mathrm{T}}\boldsymbol{H}\boldsymbol{\Gamma} \end{pmatrix} < 0 \tag{6}$$

$$\boldsymbol{\Xi}_2 = \begin{pmatrix} \boldsymbol{\Xi} + \tau_2 \boldsymbol{M}\boldsymbol{H}^{-1}\boldsymbol{M}^{\mathrm{T}} \\ + \boldsymbol{M}(\boldsymbol{e}_1 - \boldsymbol{e}_3) + (\boldsymbol{e}_1 - \boldsymbol{e}_3)^{\mathrm{T}}\boldsymbol{M}^{\mathrm{T}} \end{pmatrix} < 0 \tag{7}$$

where $\boldsymbol{\Xi} = \begin{bmatrix} \boldsymbol{\Xi}_{11} & * & * & * & * \\ \boldsymbol{\Xi}_{21} & \boldsymbol{\Xi}_{22} & * & * & * \\ \boldsymbol{\Xi}_{31} & \boldsymbol{\Xi}_{32} & \boldsymbol{\Xi}_{33} & * & * \\ 0 & \boldsymbol{\Xi}_{42} & \boldsymbol{\Xi}_{43} & \boldsymbol{\Xi}_{44} & * \\ \boldsymbol{\Xi}_{51} & 0 & \boldsymbol{\Xi}_{53} & 0 & \boldsymbol{\Xi}_{55} \end{bmatrix}$,

$\boldsymbol{\Gamma} = [\overline{\boldsymbol{A}} \quad 0 \quad \overline{\boldsymbol{B}}\boldsymbol{K} \quad 0 \quad \overline{\boldsymbol{B}}_{\varpi}]$,

$\boldsymbol{e}_1 = [\boldsymbol{I} \quad 0 \quad 0 \quad 0 \quad 0]$, $\boldsymbol{e}_3 = [0 \quad 0 \quad \boldsymbol{I} \quad 0 \quad 0]$,

$\boldsymbol{M} = [\boldsymbol{M}_1^{\mathrm{T}} \quad \boldsymbol{M}_2^{\mathrm{T}} \quad \boldsymbol{M}_3^{\mathrm{T}} \quad \boldsymbol{M}_4^{\mathrm{T}} \quad \boldsymbol{M}_5^{\mathrm{T}}]^{\mathrm{T}}$

$\boldsymbol{\Xi}_{11} = \begin{pmatrix} \overline{\boldsymbol{A}}^{\mathrm{T}}\boldsymbol{P} + \boldsymbol{P}\overline{\boldsymbol{A}} + \tau_1^2 \overline{\boldsymbol{A}}^{\mathrm{T}}\boldsymbol{R}_1\overline{\boldsymbol{A}} \\ + (\tau_2 - \tau_1)^2 \overline{\boldsymbol{A}}^{\mathrm{T}}\boldsymbol{R}_2\overline{\boldsymbol{A}} + \boldsymbol{Q}_1 - \boldsymbol{R}_1 + \overline{\boldsymbol{C}}^{\mathrm{T}}\overline{\boldsymbol{C}} \end{pmatrix}$,

$\boldsymbol{\Xi}_{21} = \boldsymbol{R}_1$, $\boldsymbol{\Xi}_{22} = \boldsymbol{Q}_2 - \boldsymbol{Q}_1 - \boldsymbol{R}_1 - \boldsymbol{R}_2$,

$\boldsymbol{\Xi}_{31} = \begin{pmatrix} \boldsymbol{K}^{\mathrm{T}}\overline{\boldsymbol{B}}^{\mathrm{T}}\boldsymbol{P} + \tau_1^2 \boldsymbol{K}^{\mathrm{T}}\overline{\boldsymbol{B}}^{\mathrm{T}}\boldsymbol{R}_1\overline{\boldsymbol{A}} \\ + (\tau_2 - \tau_1)^2 \boldsymbol{K}^{\mathrm{T}}\overline{\boldsymbol{B}}^{\mathrm{T}}\boldsymbol{R}_2\overline{\boldsymbol{A}} + \boldsymbol{K}^{\mathrm{T}}\overline{\boldsymbol{D}}^{\mathrm{T}}\overline{\boldsymbol{C}}^{\mathrm{T}} \end{pmatrix}$,

$\boldsymbol{\Xi}_{32} = -\boldsymbol{U} + \boldsymbol{R}_2$,

$\boldsymbol{\Xi}_{33} = \begin{pmatrix} \tau_1^2 \boldsymbol{K}^{\mathrm{T}}\overline{\boldsymbol{B}}^{\mathrm{T}}\boldsymbol{R}_1\overline{\boldsymbol{B}}\boldsymbol{K} + (\tau_2 - \tau_1)^2 \boldsymbol{K}^{\mathrm{T}}\overline{\boldsymbol{B}}^{\mathrm{T}}\boldsymbol{R}_2\overline{\boldsymbol{B}}\boldsymbol{K} \\ - 2\boldsymbol{R}_2 + \boldsymbol{U}^{\mathrm{T}} + \boldsymbol{U} + \boldsymbol{K}^{\mathrm{T}}\overline{\boldsymbol{D}}^{\mathrm{T}}\overline{\boldsymbol{D}}\boldsymbol{K}^{\mathrm{T}} \end{pmatrix}$,

$\boldsymbol{\Xi}_{42} = \boldsymbol{U}$, $\boldsymbol{\Xi}_{43} = -\boldsymbol{U} + \boldsymbol{R}_2$, $\boldsymbol{\Xi}_{44} = -\boldsymbol{Q}_2 - \boldsymbol{R}_2$,

$\boldsymbol{\Xi}_{51} = \overline{\boldsymbol{B}}_{\varpi}^{\mathrm{T}}\boldsymbol{P} + \tau_1^2 \overline{\boldsymbol{B}}_{\varpi}^{\mathrm{T}}\boldsymbol{R}_1\overline{\boldsymbol{A}} + (\tau_2 - \tau_1)^2 \overline{\boldsymbol{B}}_{\varpi}^{\mathrm{T}}\boldsymbol{R}_2\overline{\boldsymbol{A}}$,

$\boldsymbol{\Xi}_{53} = \tau_1^2 \overline{\boldsymbol{B}}_{\varpi}^{\mathrm{T}}\boldsymbol{R}_1\overline{\boldsymbol{B}}\boldsymbol{K} + (\tau_2 - \tau_1)^2 \overline{\boldsymbol{B}}_{\varpi}^{\mathrm{T}}\boldsymbol{R}_2\overline{\boldsymbol{B}}\boldsymbol{K}$,

$\boldsymbol{\Xi}_{55} = \tau_1^2 \overline{\boldsymbol{B}}_{\varpi}^{\mathrm{T}}\boldsymbol{R}_1\overline{\boldsymbol{B}}_{\varpi} + (\tau_2 - \tau_1)^2 \overline{\boldsymbol{B}}_{\varpi}^{\mathrm{T}}\boldsymbol{R}_2\overline{\boldsymbol{B}}_{\varpi} - \gamma^2 \boldsymbol{I}$.

**Poof** Construct a Lyapunov-Krasovskii functional candidate as $V(t, \boldsymbol{x}_t) = \sum_{i=1}^{4} V_i(t, \boldsymbol{x}_t)$, where $V_1(t, \boldsymbol{x}_t) = \boldsymbol{x}^{\mathrm{T}}(t)\boldsymbol{P}\boldsymbol{x}(t)$, $V_2(t, \boldsymbol{x}_t) = \int_{t-\tau_1}^{t} \boldsymbol{x}^{\mathrm{T}}(s)\boldsymbol{Q}_1\boldsymbol{x}(s)\mathrm{d}s + \int_{t-\tau_2}^{t-\tau_1} \boldsymbol{x}^{\mathrm{T}}(s)\boldsymbol{Q}_2\boldsymbol{x}(s)\mathrm{d}s$,

$$V_3(t, \boldsymbol{x}_t) = \begin{pmatrix} \tau_1 \int_{t-\tau_1}^{t} \int_{s}^{t} \dot{\boldsymbol{x}}^{\mathrm{T}}(v)\boldsymbol{R}_1\dot{\boldsymbol{x}}(v)\mathrm{d}v\mathrm{d}s \\ + (\tau_2 - \tau_1) \int_{t-\tau_2}^{t-\tau_1} \int_{s}^{t} \dot{\boldsymbol{x}}^{\mathrm{T}}(v)\boldsymbol{R}_2\dot{\boldsymbol{x}}(v)\mathrm{d}v\mathrm{d}s \end{pmatrix},$$

$$V_4(t, \boldsymbol{x}_t) = (\tau_2 - \tau(t)) \int_{t-\tau(t)}^{t} \dot{\boldsymbol{x}}^{\mathrm{T}}(s)\boldsymbol{H}\dot{\boldsymbol{x}}(s)\mathrm{d}s.$$

Taking the time derivative of $V(t, \boldsymbol{x}_t)$ along the trajectory of system Eq. (4) yields:

$$\dot{V}_1(t, \boldsymbol{x}_t) = 2\dot{\boldsymbol{x}}^{\mathrm{T}}(t)\boldsymbol{P}\boldsymbol{x}(t) \tag{8}$$

$$\dot{V}_2(t, \boldsymbol{x}_t) = \begin{pmatrix} \boldsymbol{x}^{\mathrm{T}}(t)\boldsymbol{Q}_1\boldsymbol{x}(t) + \boldsymbol{x}^{\mathrm{T}}(t-\tau_1)(\boldsymbol{Q}_2 - \boldsymbol{Q}_1)\boldsymbol{x}(t-\tau_1) \\ - \boldsymbol{x}^{\mathrm{T}}(t-\tau_2)\boldsymbol{Q}_2\boldsymbol{x}(t-\tau_2) \end{pmatrix} \tag{9}$$

$$\begin{aligned} \dot{V}_3(t, \boldsymbol{x}_t) = {} & \tau_1^2 \dot{\boldsymbol{x}}^{\mathrm{T}}(t)\boldsymbol{R}_1\dot{\boldsymbol{x}}(t) - \tau_1 \int_{t-\tau_1}^{t} \dot{\boldsymbol{x}}^{\mathrm{T}}(s)\boldsymbol{R}_1\dot{\boldsymbol{x}}(s)\mathrm{d}s \\ & + (\tau_2 - \tau_1)^2 \dot{\boldsymbol{x}}^{\mathrm{T}}(t)\boldsymbol{R}_2\dot{\boldsymbol{x}}(t) \\ & - (\tau_2 - \tau_1) \int_{t-\tau_2}^{t-\tau_1} \dot{\boldsymbol{x}}^{\mathrm{T}}(s)\boldsymbol{R}_2\dot{\boldsymbol{x}}(s)\mathrm{d}s \end{aligned} \tag{10}$$

$$\begin{aligned} \dot{V}_4(t, \boldsymbol{x}_t) = {} & - \int_{t-\tau(t)}^{t} \dot{\boldsymbol{x}}^{\mathrm{T}}(s)\boldsymbol{H}\dot{\boldsymbol{x}}(s)\mathrm{d}s \\ & + (\tau_2 - \tau(t))\dot{\boldsymbol{x}}^{\mathrm{T}}(\mathrm{t})\boldsymbol{H}\dot{\boldsymbol{x}}(t) \end{aligned} \tag{11}$$

Utilizing Lemma 1 to deal with integral items in Eq. (10), the following is obtained:

$$\begin{aligned} & -\tau \int_{t-\tau_1}^{t} \dot{\boldsymbol{x}}^{\mathrm{T}}(s)\boldsymbol{R}_1\dot{\boldsymbol{x}}(s)\mathrm{d}s \\ & \leqslant - [\boldsymbol{x}^{\mathrm{T}}(t) \quad \boldsymbol{x}^{\mathrm{T}}(t-\tau_1)] \begin{bmatrix} \boldsymbol{R}_1 & * \\ -\boldsymbol{R}_1 & \boldsymbol{R}_1 \end{bmatrix} \begin{bmatrix} \boldsymbol{x}(t) \\ \boldsymbol{x}(t-\tau_1) \end{bmatrix} \end{aligned} \tag{12}$$

For a matrix $\boldsymbol{U}$ satisfying Eq. (5) the following is got and by utilizing Lemma 2:

$$\begin{aligned} & -(\tau_2 - \tau_1) \int_{t-\tau_2}^{t-\tau_1} \dot{\boldsymbol{x}}^{\mathrm{T}}(\mathrm{s})\boldsymbol{R}_2\dot{\boldsymbol{x}}(s)\mathrm{d}s \\ & \leqslant - \left\{ \begin{aligned} & \boldsymbol{x}^{\mathrm{T}}(t-\tau_1)\boldsymbol{R}_2\boldsymbol{x}(t-\tau_1) \\ & + \boldsymbol{x}^{\mathrm{T}}(t-\tau_1)(\boldsymbol{U}^{\mathrm{T}} - \boldsymbol{R}_2)\boldsymbol{x}(t-\tau(t)) \\ & - \boldsymbol{x}^{\mathrm{T}}(t-\tau_1)\boldsymbol{U}^{\mathrm{T}}\boldsymbol{x}(t-\tau_2) \\ & + \boldsymbol{x}^{\mathrm{T}}(t-\tau(t))(\boldsymbol{U} - \boldsymbol{R}_2)\boldsymbol{x}(t-\tau_1) \\ & + \boldsymbol{x}^{\mathrm{T}}(t-\tau(t))(2\boldsymbol{R}_2 - \boldsymbol{U}^{\mathrm{T}} - \boldsymbol{U})\boldsymbol{x}(t-\tau(t)) \\ & + \boldsymbol{x}^{\mathrm{T}}(t-\tau(t))(\boldsymbol{U}^{\mathrm{T}} - \boldsymbol{R}_2)\boldsymbol{x}(t-\tau_2) \\ & - \boldsymbol{x}^{\mathrm{T}}(t-\tau_2)\boldsymbol{U}\boldsymbol{x}(t-\tau_1) \\ & + \boldsymbol{x}^{\mathrm{T}}(t-\tau_2)(\boldsymbol{U} - \boldsymbol{R}_2)\boldsymbol{x}(t-\tau(t)) \\ & + \boldsymbol{x}^{T}(t-\tau_2)\boldsymbol{R}_2\boldsymbol{x}(t-\tau_2) \end{aligned} \right\} \end{aligned} \tag{13}$$

Then, using the Newton-Leibniz formula and a free weighting matrix $\boldsymbol{M}$ with appropriate dimensions, it is clear that:

$$2\boldsymbol{\xi}^{\mathrm{T}}(t)\boldsymbol{M}\left[\boldsymbol{x}(t)-\boldsymbol{x}(t-\tau(t))-\int_{t-\tau(t)}^{t}\dot{\boldsymbol{x}}(s)\mathrm{d}s\right]=0 \tag{14}$$

where

$\boldsymbol{\xi}^{\mathrm{T}}(t)=$
$[\boldsymbol{x}^{\mathrm{T}}(t)\ \ \boldsymbol{x}^{\mathrm{T}}(t-\tau_1)\ \ \boldsymbol{x}^{\mathrm{T}}(t-\tau(t))\ \ \boldsymbol{x}^{\mathrm{T}}(t-\tau_2)\ \ \boldsymbol{\omega}(t)]$.

By using Cauchy inequality, one can easily obtain

$$-2\boldsymbol{\xi}^{\mathrm{T}}(t)\boldsymbol{M}\int_{t-\tau(t)}^{t}\dot{\boldsymbol{x}}(s)\mathrm{d}s\leqslant\begin{pmatrix}\tau(t)\boldsymbol{\xi}^{\mathrm{T}}(t)\boldsymbol{M}\boldsymbol{H}^{-1}\boldsymbol{M}^{\mathrm{T}}\boldsymbol{\xi}(t)\\+\int_{t-\tau(t)}^{t}\dot{\boldsymbol{x}}^{\mathrm{T}}(s)\boldsymbol{H}\dot{\boldsymbol{x}}(s)\mathrm{d}s\end{pmatrix} \tag{15}$$

Combining Eqs(8) – (15) together, there is

$$\begin{aligned}&\dot{V}(t)+\boldsymbol{e}^{\mathrm{T}}(t)\boldsymbol{e}(t)-\gamma^2\varpi^{T}(t)\varpi(t)\\&\leqslant\boldsymbol{\xi}^{\mathrm{T}}(t)\begin{bmatrix}\boldsymbol{\Xi}+\tau(t)\boldsymbol{M}\boldsymbol{H}^{-1}\boldsymbol{M}^{\mathrm{T}}+2\boldsymbol{M}(\boldsymbol{e}_1-\boldsymbol{e}_3)\\+(\tau_2-\tau(t))\boldsymbol{\Gamma}^{\mathrm{T}}\boldsymbol{H}\boldsymbol{\Gamma}\end{bmatrix}\boldsymbol{\xi}(t)\end{aligned} \tag{16}$$

where $\boldsymbol{\Gamma}=[\bar{\boldsymbol{A}}\ \ 0\ \ \bar{\boldsymbol{B}}\boldsymbol{K}\ \ 0\ \ \bar{\boldsymbol{B}}_{\varpi}]$, $\boldsymbol{e}_1=[\boldsymbol{I}\ \ 0\ \ 0\ \ 0\ \ 0]$, $\boldsymbol{e}_3=[0\ \ 0\ \ \boldsymbol{I}\ \ 0\ \ 0]$.

When the conditions Eqs(6) – (7) in Theorem 1 are hold, $[\boldsymbol{\Xi}+\tau(t)\boldsymbol{M}\boldsymbol{H}^{-1}\boldsymbol{M}^{\mathrm{T}}+2\boldsymbol{M}(\boldsymbol{e}_1-\boldsymbol{e}_3)+(\tau_2-\tau(t))\boldsymbol{\Gamma}^{\mathrm{T}}\boldsymbol{H}\boldsymbol{\Gamma}]<0$ can be concluded by applying Lemma 3. So $\dot{V}(t)<\gamma^2\varpi^{\mathrm{T}}(t)\varpi(t)-\boldsymbol{e}^{\mathrm{T}}(t)\boldsymbol{e}(t)$ could be got. When $\varpi(t)=0$, the system is obviously asymptotically stable; when $\varpi(t)\neq0$, it can be concluded $\|\boldsymbol{e}(t)\|_2<\gamma^2\|\varpi(t)\|_2$ for all nonzero $\varpi(t)$ with the zero initial condition. The proof is completed.

**Remark 3** In the stability analysis of time-delay systems, the Jensen's inequality and reciprocally convex approach have played a very important role in the existing research results. However, it is very difficult for them to take advantage of the information of the well-known sawtooth delay $\tau(t)$, which limits the further reduction of the stability condition. Therefore, $V_4(t)=(\tau_2-\tau(t))\int_{t-\tau(t)}^{t}\dot{\boldsymbol{x}}^{\mathrm{T}}(s)\boldsymbol{H}\dot{\boldsymbol{x}}(s)\mathrm{d}s$ is introduced to exploit the available information on the derivative of the delay by the free-weighting matrices method $\tau(t)$ in this paper.

## 3 H∞ output tracking controller design

In this section, the problem of $H\infty$ output tracking controller is solved based on Theorem 1.

**Lemma 4**[34] Given appropriately dimensioned matrices $\boldsymbol{W}$, $\boldsymbol{D}$ $\boldsymbol{E}$ with $\boldsymbol{W}=\boldsymbol{W}^{\mathrm{T}}$, then $\boldsymbol{W}+\boldsymbol{D}\boldsymbol{F}(t)\boldsymbol{E}+\boldsymbol{E}^{\mathrm{T}}\boldsymbol{F}^{\mathrm{T}}(t)\boldsymbol{D}^{\mathrm{T}}<0$ holds for $\boldsymbol{F}(t)$ satisfying $\boldsymbol{F}^{\mathrm{T}}(t)\boldsymbol{F}(t)\leqslant\boldsymbol{I}$, if and only if there exists a positive constant $\varepsilon$, such that:

$$\boldsymbol{W}+\varepsilon\boldsymbol{D}\boldsymbol{D}^{\mathrm{T}}+\varepsilon^{-1}\boldsymbol{E}^{\mathrm{T}}\boldsymbol{E}<0$$

**Theorem 2** For given scalars $\gamma$, $\tau_1$ and $\tau_2$, the augmented closed-loop system Eq. (4) is asymptotically stable and can achieve the $H\infty$ output tracking performance $\gamma$, if there exist scalars $\varepsilon$, $\beta$, and matrices $\boldsymbol{X}>0$, $\boldsymbol{Y}>0$, $\tilde{\boldsymbol{Q}}_1>0$, $\tilde{\boldsymbol{Q}}_2>0$, $\tilde{\boldsymbol{R}}_1>0$, $\tilde{\boldsymbol{R}}_2>0$, $\tilde{\boldsymbol{H}}>0$, $\tilde{\boldsymbol{M}}$, $\tilde{\boldsymbol{U}}$ with appropriate dimensions such that:

$$\begin{bmatrix}\tilde{\boldsymbol{R}}_2 & *\\ \tilde{\boldsymbol{U}} & \tilde{\boldsymbol{R}}_2\end{bmatrix}>0 \tag{17}$$

$$\begin{bmatrix}
\boldsymbol{\Psi}_{11} & * & * & * & * & * & * & * & * & * & * & * & * & *\\
\boldsymbol{\Psi}_{21} & \boldsymbol{\Psi}_{22} & * & * & * & * & * & * & * & * & * & * & * & *\\
\boldsymbol{\Psi}_{31} & \boldsymbol{\Psi}_{23} & \boldsymbol{\Psi}_{33} & * & * & * & * & * & * & * & * & * & * & *\\
\boldsymbol{\Psi}_{41} & \boldsymbol{\Psi}_{24} & \boldsymbol{\Psi}_{43} & \boldsymbol{\Psi}_{44} & * & * & * & * & * & * & * & * & * & *\\
\boldsymbol{\Psi}_{51} & 0 & \boldsymbol{\Psi}_{53} & 0 & \boldsymbol{\Psi}_{55} & * & * & * & * & * & * & * & * & *\\
\boldsymbol{\Psi}_{61} & \boldsymbol{\Psi}_{26} & \boldsymbol{\Psi}_{63} & \boldsymbol{\Psi}_{64} & \boldsymbol{\Psi}_{65} & \boldsymbol{\Psi}_{66} & * & * & * & * & * & * & * & *\\
\boldsymbol{\Psi}_{71} & 0 & \boldsymbol{\Psi}_{73} & 0 & \boldsymbol{\Psi}_{75} & 0 & \boldsymbol{\Psi}_{77} & * & * & * & * & * & * & *\\
\boldsymbol{\Psi}_{81} & 0 & \boldsymbol{\Psi}_{83} & 0 & \boldsymbol{\Psi}_{85} & 0 & 0 & \boldsymbol{\Psi}_{88} & * & * & * & * & * & *\\
\boldsymbol{\Psi}_{91} & 0 & \boldsymbol{\Psi}_{93} & 0 & \boldsymbol{\Psi}_{95} & 0 & 0 & 0 & \boldsymbol{\Psi}_{99} & * & * & * & * & *\\
\boldsymbol{\Psi}_{101} & 0 & 0 & 0 & 0 & 0 & \boldsymbol{\Psi}_{107} & \boldsymbol{\Psi}_{108} & \boldsymbol{\Psi}_{109} & \boldsymbol{\Psi}_{1010} & * & * & * & *\\
\boldsymbol{\Psi}_{111} & 0 & \boldsymbol{\Psi}_{113} & 0 & 0 & 0 & 0 & 0 & 0 & 0 & \boldsymbol{\Psi}_{1111} & * & * & *\\
\boldsymbol{\Psi}_{121} & 0 & \boldsymbol{\Psi}_{123} & 0 & 0 & 0 & 0 & 0 & 0 & 0 & 0 & \boldsymbol{\Psi}_{1212} & * & *\\
0 & 0 & 0 & 0 & 0 & 0 & 0 & 0 & 0 & 0 & 0 & \boldsymbol{\Psi}_{1312} & \boldsymbol{\Psi}_{1313} & *\\
\boldsymbol{\Psi}_{141} & 0 & \boldsymbol{\Psi}_{143} & 0 & 0 & 0 & 0 & 0 & 0 & 0 & 0 & 0 & 0 & \boldsymbol{\Psi}_{1414}
\end{bmatrix}<0 \tag{18}$$

$$\begin{bmatrix} \Theta_{11} & * & * & * & * & * & * & * & * & * & * & * & * \\ \Theta_{21} & \Theta_{22} & * & * & * & * & * & * & * & * & * & * & * \\ \Theta_{31} & \Theta_{32} & \Theta_{33} & * & * & * & * & * & * & * & * & * & * \\ \Theta_{41} & \Theta_{42} & \Theta_{43} & \Theta_{44} & * & * & * & * & * & * & * & * & * \\ \Theta_{51} & 0 & \Theta_{53} & 0 & \Theta_{55} & * & * & * & * & * & * & * & * \\ \Theta_{61} & \Theta_{62} & \Theta_{63} & \Theta_{64} & \Theta_{65} & \Theta_{66} & * & * & * & * & * & * & * \\ \Theta_{71} & 0 & \Theta_{73} & 0 & \Theta_{75} & 0 & \Theta_{77} & * & * & * & * & * & * \\ \Theta_{81} & 0 & \Theta_{83} & 0 & \Theta_{85} & 0 & 0 & \Theta_{88} & * & * & * & * & * \\ \Theta_{91} & 0 & 0 & 0 & 0 & 0 & \Theta_{97} & \Theta_{98} & \Theta_{99} & * & * & * & * \\ \Theta_{101} & 0 & \Theta_{103} & 0 & 0 & 0 & 0 & 0 & 0 & \Theta_{1010} & * & * & * \\ \Theta_{111} & 0 & \Theta_{113} & 0 & 0 & 0 & 0 & 0 & 0 & 0 & \Theta_{1111} & * & * \\ 0 & 0 & 0 & 0 & 0 & 0 & 0 & 0 & 0 & 0 & \Theta_{1211} & \Theta_{1212} & * \\ \Theta_{131} & 0 & \Theta_{123} & 0 & 0 & 0 & 0 & 0 & 0 & 0 & 0 & 0 & \Theta_{1313} \end{bmatrix} \leqslant 0 \quad (19)$$

where

$\Theta_{11} = \Psi_{11} = XA^{\mathrm{T}} + AX + \tilde{Q}_1 - \tilde{R}_1 + \tilde{M}_1 + \tilde{M}_1^{\mathrm{T}}$,
$\Theta_{21} = \Psi_{21} = \tilde{R}_1 + \tilde{M}_2$,
$\Theta_{22} = \Psi_{22} = \tilde{Q}_2 - \tilde{Q}_1 - \tilde{R}_1 - \tilde{R}_2$,
$\Theta_{31} = \Psi_{31} = Y^{\mathrm{T}}B^{\mathrm{T}} + \tilde{M}_3 - \tilde{M}_1^{\mathrm{T}}$,
$\Theta_{32} = \Psi_{32} = -\tilde{U} + \tilde{R}_2 - \tilde{M}_2^{\mathrm{T}}$,
$\Theta_{33} = \Psi_{33} = -2\tilde{R}_2 + \tilde{U}^{\mathrm{T}} + \tilde{U} - \tilde{M}_3 - \tilde{M}_3^{\mathrm{T}}$,
$\Theta_{41} = \Psi_{41} = \tilde{M}_4$, $\Theta_{42} = \Psi_{42} = \tilde{U}$, $\Theta_{44} = -\tilde{Q}_2 - \tilde{R}_2$,
$\Theta_{51} = \Psi_{51} = \bar{B}_{\varpi}^{\mathrm{T}} + \tilde{M}_5$, $\Theta_{53} = \Psi_{53} = -\tilde{M}_5$,
$\Theta_{55} = \Psi_{55} = -\gamma^2$,
$\Theta_{61} = \sqrt{\tau_2}\tilde{M}_1^{\mathrm{T}}$, $\Theta_{62} = \sqrt{\tau_2}\tilde{M}_2^{\mathrm{T}}$, $\Theta_{63} = \sqrt{\tau_2}\tilde{M}_3^{\mathrm{T}}$,
$\Theta_{64} = \sqrt{\tau_2}\tilde{M}_4^{\mathrm{T}}$, $\Theta_{65} = \sqrt{\tau_2}\tilde{M}_5^{\mathrm{T}}$, $\Psi_{61} = \sqrt{\tau_1}\tilde{M}_1^{\mathrm{T}}$,
$\Psi_{62} = \sqrt{\tau_1}\tilde{M}_2^{\mathrm{T}}$, $\Psi_{63} = \sqrt{\tau_1}\tilde{M}_3^{\mathrm{T}}$, $\Psi_{64} = \sqrt{\tau_1}\tilde{M}_4^{\mathrm{T}}$,
$\Psi_{65} = \sqrt{\tau_1}\tilde{M}_5^{\mathrm{T}}$, $\Theta_{66} = \Psi_{66} = -\tilde{H}$,
$\Theta_{71} = \Psi_{71} = \tau_1 AX$, $\Theta_{73} = \Psi_{73} = \tau_1 BY$,
$\Theta_{75} = \Psi_{75} = \tau_1 \bar{B}_{\varpi}$,
$\Theta_{77} = \Psi_{77} = -X\tilde{R}_1^{-1}X$, $\Theta_{81} = \Psi_{81} = (\tau_2 - \tau_1)\mathbf{AX}$,
$\Theta_{83} = \Psi_{83} = (\tau_2 - \tau_1)BY$,
$\Theta_{85} = \Psi_{85} = (\tau_2 - \tau_1)\bar{B}_{\varpi}$,
$\Theta_{88} = \Psi_{88} = -X\tilde{R}_2^{-1}X$, $\Psi_{91} = \sqrt{(\tau_2 - \tau_1)}AX$,
$\Psi_{93} = \sqrt{(\tau_2 - \tau_1)}BY$, $\Psi_{95} = -\sqrt{(\tau_2 - \tau_1)}\bar{B}_{\varpi}$,
$\Psi_{99} = -X\tilde{H}^{-1}X$,
$\Theta_{91} = \Psi_{101} = \varepsilon G^{\mathrm{T}}$, $\Theta_{97} = \Psi_{107} = \tau_1 \varepsilon G^{\mathrm{T}}$,
$\Theta_{98} = \Psi_{108} = (\tau_2 - \tau_1)\varepsilon G^{\mathrm{T}}$, $\Psi_{109} = \sqrt{(\tau_2 - \tau_1)}\varepsilon G^{\mathrm{T}}$,
$\Theta_{99} = \Psi_{1010} = -\varepsilon I$, $\Theta_{101} = \Psi_{111} = E_a X$,
$\Theta_{103} = \Psi_{113} = E_b Y$, $\Theta_{1010} = \Psi_{1111} = -\varepsilon I$,
$\Theta_{111} = \Psi_{121} = CX$, $\Theta_{113} = \Psi_{123} = DY$,
$\Theta_{1111} = \Psi_{1212} = -I$, $\Theta_{1211} = \Psi_{1312} = \beta N^{\mathrm{T}}$,
$\Theta_{1212} = \Psi_{1313} = -\beta I$, $\Theta_{131} = \Psi_{141} = E_c X$,
$\Theta_{133} = \Psi_{143} = E_d Y$, $\Theta_{1313} = \Psi_{1414} = -\beta I$,
$\tilde{M} = [\tilde{M}_1^{\mathrm{T}} \quad \tilde{M}_2^{\mathrm{T}} \quad \tilde{M}_3^{\mathrm{T}} \quad \tilde{M}_4^{\mathrm{T}} \quad \tilde{M}_5^{\mathrm{T}}]^{\mathrm{T}}$.

Moreover, the gain matrix of the designed controller in Eq. (3) can be obtained by $K = YX^{-1}$.

**Poof** Because of $\| F_p^{\mathrm{T}}(t)F_p(t) \|_2 < I$ and $\| \Delta_p^{\mathrm{T}}(t)\Delta_p(t) \|_2 < I$, the uncertainty terms $F_p(t)$ and $\Delta_p(t)$ can be eliminated by applying Lemma 4 and Schur complement to Eq. (6). Then, by pre- and post-multiplying both sides of the resulting inequality with $diag(X, X, X, X, I, R_1^{-1}, R_2^{-1}, H^{-1}, I, I, I, I, I)$ and its trans-pose respectively, where $X = P^{-1}$. Define $Y = KX$, $\tilde{Q}_1 = XQ_1X$, $\tilde{Q}_2 = XQ_2X$, $\tilde{R}_1 = X\tilde{R}_1X$, $\tilde{R}_2 = X\tilde{R}_2X$, and $\tilde{M} = [(XM_1X)^{\mathrm{T}} \quad (XM_2X)^{\mathrm{T}} \quad (XM_3X)^{\mathrm{T}} \quad (XM_4X)^{\mathrm{T}} \quad (M_5X)^{\mathrm{T}}]^{\mathrm{T}}$, Eq. (18) can be readily reached. In addition, Eq. (17) can be obtained by pre- and post-multiplying both sides of Eq. (5) with $diag\{X, X\}$ and its transpose respectively. As the process of Eq. (17), Eq. (19) can be obtained from Eq. (7), which completes the proof.

Note that Theorem 2 contains some nonlinear terms, such as $X\tilde{R}_1^{-1}X$, $X\tilde{R}_2^{-1}X$, and $XH^{-1}X$. Therefore, LMIs can't be used directly to solve Theorem 2.

**Remark 4** There are generally two methods to deal with the nonlinear term in Theorem 2: (1) Use the bounding inequalities $-X\tilde{H}^{-1}X \leqslant \tilde{H}^{-1} - 2X$, $-X\tilde{R}_i^{-1}X \leqslant \tilde{R}_i^{-1} - 2X$, $(i = 1,2)$ to transform nonlinear matrix inequalities into LMIs. (2) Use the modified cone complementary linearization (CCL) algorithm. For the bounding inequalities, if $\tilde{H}^{-1}$, $\tilde{R}_i^{-1}$ and $X$ with $\alpha_i^2\tilde{H}^{-1}$, $\alpha_i^2\tilde{R}_i^{-1}$ and $\alpha_i X$ are replaced respectively, the inequalities $-X\tilde{H}^{-1}X \leqslant \alpha_i^2\tilde{H}^{-1} - 2\alpha_i X$, $-X\tilde{R}_i^{-1}X \leqslant \alpha_i^2\tilde{R}_i^{-1} - 2\alpha_i X$, $(i = 1,2)$ will be obtained which will introduce less conservativeness with additional parameters $\alpha_i$. By using the cone complementary linearization (CCL) algorithm, the nonlinear matrix in Theorem 2 could be changed to a minimization problem subject to LMIs. The method (2) would be a better choice relative to mothod (1) if one can afford more computational efforts[35].

In order to solve the controller gain by LMI tools and obtain less conservativeness by CCL as in Ref. [35], the conditions in Theorem 2 needs to be further converted. First of all, assume that the matrixes $\boldsymbol{L}_1 > 0$, $\boldsymbol{L}_2 > 0$, $\boldsymbol{L}_3 > 0$ satisfy:

$$-\boldsymbol{L}_3 \geqslant -\boldsymbol{X}\tilde{\boldsymbol{H}}^{-1}\boldsymbol{X},\ -\boldsymbol{L}_i \geqslant -\boldsymbol{X}\tilde{\boldsymbol{R}}_i^{-1}\boldsymbol{X},\ i = 1,2 \tag{20}$$

Then Eq. (21) can be obtained by using Schur complement to Eq. (20).

$$\begin{bmatrix} -\tilde{\boldsymbol{H}}^{-1} & \boldsymbol{X}^{-1} \\ \boldsymbol{X}^{-1} & -\boldsymbol{L}_3^{-1} \end{bmatrix} \leqslant 0, \begin{bmatrix} -\tilde{\boldsymbol{R}}_i^{-1} & \boldsymbol{X}^{-1} \\ \boldsymbol{X}^{-1} & -\boldsymbol{L}_i^{-1} \end{bmatrix} \leqslant 0,\quad i = 1,2 \tag{21}$$

Introducing new variables $\boldsymbol{X}_N$, $\boldsymbol{H}_N$, $\boldsymbol{R}_{1N}$, $\boldsymbol{R}_{2N}$, $\boldsymbol{L}_{1N}$, $\boldsymbol{L}_{2N}$ and $\boldsymbol{L}_{3N}$, Eq. (21) can be rewritten into Eqs(22) - (23).

$$\begin{bmatrix} -\tilde{\boldsymbol{H}}_N & \boldsymbol{X}_N \\ \boldsymbol{X}_N & -\boldsymbol{L}_{3N} \end{bmatrix} \leqslant 0, \begin{bmatrix} -\tilde{\boldsymbol{R}}_{iN} & \boldsymbol{X}_N \\ \boldsymbol{X}_N & -\boldsymbol{L}_{iN} \end{bmatrix} \leqslant 0,\quad i = 1,2 \tag{22}$$

$$\begin{aligned} &\boldsymbol{X}\boldsymbol{X}_N = \boldsymbol{I},\ \tilde{\boldsymbol{R}}_1\tilde{\boldsymbol{R}}_{1N} = \boldsymbol{I},\ \tilde{\boldsymbol{R}}_2\tilde{\boldsymbol{R}}_{2N} = \boldsymbol{I}, \\ &\tilde{\boldsymbol{H}}\tilde{\boldsymbol{H}}_N = \boldsymbol{I},\ \boldsymbol{L}_1\boldsymbol{L}_{1N} = \boldsymbol{I},\ \boldsymbol{L}_2\boldsymbol{L}_{2N} = \boldsymbol{I},\ \boldsymbol{L}_3\boldsymbol{L}_{3N} = \boldsymbol{I} \end{aligned} \tag{23}$$

Therefore, Theorem 2 could be changed to a minimization problem subject to LMIs. Minimize $tr(\boldsymbol{X}\boldsymbol{X}_n + \tilde{\boldsymbol{R}}_1\tilde{\boldsymbol{R}}_{1N} + \tilde{\boldsymbol{R}}_2\tilde{\boldsymbol{R}}_{2N} + \tilde{\boldsymbol{H}}\tilde{\boldsymbol{H}}_N + \sum_{i=1}^{3}\boldsymbol{L}_i\boldsymbol{L}_{iN})$ subject to Eqs(18) - (19), (22), $\begin{bmatrix} \boldsymbol{X} & * \\ 0 & \boldsymbol{X}_N \end{bmatrix} > 0$, $\begin{bmatrix} \boldsymbol{R}_i & * \\ 0 & \boldsymbol{R}_{iN} \end{bmatrix} > 0$, $i = 1,2$

and $\begin{bmatrix} \boldsymbol{H} & * \\ 0 & \boldsymbol{H}_N \end{bmatrix} > 0$, $\begin{bmatrix} \boldsymbol{L}_j & * \\ 0 & \boldsymbol{L}_{jN} \end{bmatrix} > 0$, $j = 1,2,3$

where nonlinear terms $\boldsymbol{X}\tilde{\boldsymbol{R}}_1^{-1}\boldsymbol{X}$, $\boldsymbol{X}\tilde{\boldsymbol{R}}_2^{-1}\boldsymbol{X}$ and $\boldsymbol{X}\boldsymbol{H}^{-1}\boldsymbol{X}$ are replaced by $\boldsymbol{L}_1$, $\boldsymbol{L}_2$, $\boldsymbol{L}_3$ respectively in Eqs(18) - (19). Then the control gain $\boldsymbol{K} = \boldsymbol{Y}\boldsymbol{X}^{-1}$ can be obtained.

## 4 Numerical examples

Firstly, this section uses the DC motor system of Quanser robot to illustrate the effectiveness of the proposed approach for robust output tracking control of NCSs with network-induced delays, packet dropouts, parameter uncertainties and external disturbances. Then, by comparing with the results in Refs[17,19,21,22], the second example illustrates the proposed $H\infty$ performance criterion can yield the less conservative result. Lastly, the third example concerns the $H\infty$ output tracking control design problem for an actual satellite system, and verifies the advantages by a simulation scenario.

**Example 1** Consider the DC motor system of Quanser robot. The DC motor armature circuit schematic and gear train are illustrated in Fig. 2. Its voltage-to-position transfer function Eq. (24) can be derived from classical mechanics principles and using experimental methods.

$$\frac{\theta_l(s)}{V_i(s)} = \frac{\eta_g K_g \eta_m k_t}{s(R_m(\eta_g K_g^2 J_m + J_l)s + \eta_g K_g^2 \eta_m k_t k_m + R_m \eta_g K_g^2 B_m + R_m B_l)} \tag{24}$$

here, $R_m$ is the motor resistance, $K_t$ is the current-torque constant, $\eta_m$ is the motor efficiency, $K_m$ is the back-emf constant, $K_g$ Kg is the gear ratio, $\eta_g$ is the gearbox efficiency, $J_m$ is the motor shaft moment of inertia, $J_l$ is the moment of inertia of the load, $B_m$ is the viscous friction acting on the motor shaft, and $B_l$ is the viscous friction acting on the load shaft . Using the system specifications given by Quanser, the voltage-to-position transfer function $\frac{\theta_l(s)}{V_i(s)} = \frac{b_0}{s^2 + a_1 s}$ can be obtained, where $a_1 = 24.15$, $b_0 = 36.96$. One possible state-space realization Eq. (25) for the transfer function can be obtained:

$$\begin{aligned} \dot{\boldsymbol{x}}(t) &= \boldsymbol{A}\boldsymbol{x}(t) + \boldsymbol{B}\boldsymbol{u}(t) + \boldsymbol{B}_\omega\boldsymbol{\omega}(t) \\ \boldsymbol{y}(t) &= \boldsymbol{C}\boldsymbol{x}(t) \end{aligned} \tag{25}$$

where $\boldsymbol{A} = \begin{bmatrix} 0 & 1 \\ 0 & -a_1 + r(t) \end{bmatrix}$, $\boldsymbol{B} = \begin{bmatrix} 0 \\ b_0 + s(t) \end{bmatrix}$, $\boldsymbol{B}_w = \begin{bmatrix} 0 \\ b_\omega \end{bmatrix}$, $\boldsymbol{C} = [1 \quad 0]$, $r(t)$ and $s(t)$ are the errors of the modeling. According to model Eq. (1), $\boldsymbol{A}_p = \begin{bmatrix} 0 & 1 \\ 0 & -24.15 \end{bmatrix}$, $\boldsymbol{B}_p = \begin{bmatrix} 0 \\ 36.96 \end{bmatrix}$, $\boldsymbol{C}_p = [1 \quad 0]$ can be obtained. Next, the tracking performance of the system for different uncertainties of parameters and disturbance input matrices $\boldsymbol{B}_\omega$ will be studied respectively.

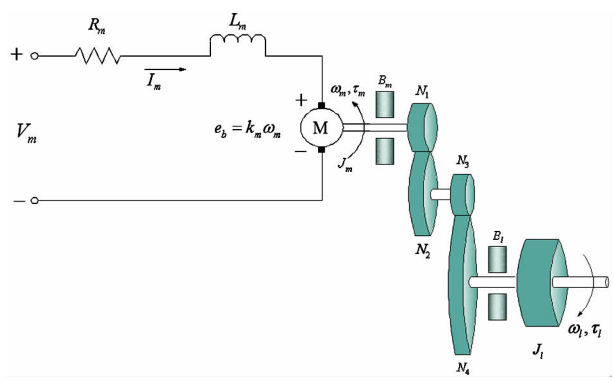


**Fig. 2** DC motor armature circuit and gear train

The reference model is described as follows:

$$\begin{cases} \dot{\boldsymbol{x}}_r(t) = -\boldsymbol{x}_r(t) + \boldsymbol{r}(t) \\ \boldsymbol{y}_r(t) = 0.5\boldsymbol{x}_r(t) \end{cases} \tag{26}$$

Assuming that the system model is time-invariant, the performance of the system under different disturbance input matrices $\boldsymbol{B}_\omega$ is analyzed. The results are shown in Table 1.

Table 1 Minimum value of $\gamma$ and $\boldsymbol{K}$ for different $\boldsymbol{B}_\omega$

| $\boldsymbol{B}_\omega$ | $\gamma$ | $\boldsymbol{K}$ |
|---|---|---|
| $[0 \quad 0]^T$ | 0.055 | $[-12.9840 \quad -0.5767 \quad 6.3553]$ |
| $[0 \quad 3]^T$ | 0.056 | $[-12.8433 \quad -0.5750 \quad 6.2728]$ |
| $[0 \quad 10]^T$ | 0.064 | $[-11.9483 \quad -0.5040 \quad 5.9049]$ |
| $[0 \quad 20]^T$ | 0.088 | $[-10.0768 \quad -0.2803 \quad 5.0873]$ |
| $[0 \quad 36.96]^T$ | 0.141 | $[-10.0768 \quad -0.2803 \quad 5.0873]$ |

When $\boldsymbol{B}_\omega = [0 \quad 10]^{\mathrm{T}}$, the performance of the system, under the different uncertain parameters which change in the range of 5%, 10%, 15% and 20%, respectively, is also analyzed. Base on the uncertainties, the matrices $\boldsymbol{F}_p(t) = \begin{bmatrix} 0 & 0 \\ 0 & 0.98 \times \cos t \end{bmatrix}$, $\boldsymbol{G}_p = \begin{bmatrix} 0 & 0 \\ 0 & 1.9 \end{bmatrix}$, $\boldsymbol{E}_{pa} = \begin{bmatrix} 0 & 0 \\ 0 & 0.65 \times i \end{bmatrix}$ and $\boldsymbol{E}_{pb} = \begin{bmatrix} 0 \\ i \end{bmatrix}$ can be set, where $i = 1,2,3,4$ for 5%, 10%, 15% and 20%. According to Theorem 2, the performance index and controller gain can be got correspondingly, as shown in Table 2.

Table 2 Minimum value of $\gamma$ and $\boldsymbol{K}$ for different parameter uncertainties

| Uncertainties of parameters | $\gamma$ | $\boldsymbol{K}$ |
|---|---|---|
| 0 | 0.055 | $[-12.9840 \quad -0.5767 \quad 6.3553]$ |
| 5% | 0.069 | $[-11.7625 \quad -0.4746 \quad 5.7214]$ |
| 10% | 0.075 | $[-11.7809 \quad -0.4528 \quad 5.6287]$ |
| 15% | 0.81 | $[-11.5014 \quad -0.4216 \quad 5.3751]$ |
| 20% | 0.88 | $[-10.8374 \quad -0.3726 \quad 4.9848]$ |

When the uncertainty of parameters is 20% and $\boldsymbol{B}_\omega = [0 \quad 36.96]^{\mathrm{T}}$, it is colluded that the minimum value of $\gamma$ is 0.204 and $\boldsymbol{K} = [-8.8997 \quad -0.2438 \quad 3.9532]$.

Assuming the sampling period is $h = 15$ ms, the network induced delays is $\tau_k \in (5\text{ ms}, \quad h)$, and the upper bound of consecutive packet dropouts is $\bar{d} = 2$. So, $\tau_1 = 5$ ms and $\tau_2 = 60$ ms can be concluded.

For simulation purpose, set $\boldsymbol{\omega}(t) = 0.1\sin(5t)$, and $\boldsymbol{r}(t) = 5\sin(t)$. The initial conditions of the system are set as $\boldsymbol{x}(t) = [0 \quad 0]^{\mathrm{T}}$ and $\boldsymbol{x}_r(t) = 0$, respectively. Suppose the packet dropouts sequence is [011011011…011011], where 0 represents no packet dropouts, while 1 represents packet dropouts, the simulation results in the following three cases, as shown in Fig. 3, are used to illustrate the effectiveness of the proposed algorithm. Case 1: The system model is time-invariant and $\boldsymbol{B}_\omega = [0 \quad 0]^{\mathrm{T}}$. Case 2: The uncertainty of parameters is 15% and $\boldsymbol{B}_\omega = [0 \quad 10]^{\mathrm{T}}$. Case 3: The uncertainty of parameters is 20% and $\boldsymbol{B}_\omega = [0 \quad 36.96]^{\mathrm{T}}$.

It can be clearly seen that the system has a good output tracking trajectory, whenever the system suffers from parameter uncertainties, external disturbances, network-induced delays and serious packet dropouts.

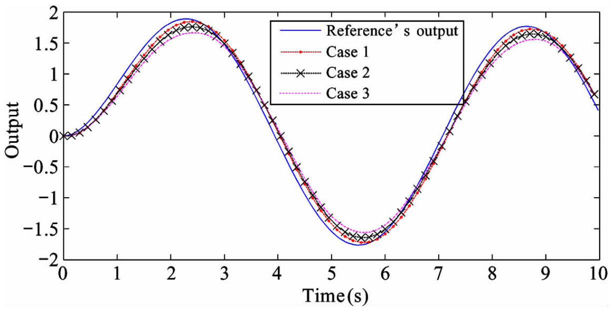


**Fig. 3** Reference's output $y_r(t)$ and system's outputs $y(t)$ for different cases (Example)

**Example 2** Consider the system model parameters with no uncertainties in Refs[17, 19], $\boldsymbol{A}_p = \begin{bmatrix} 0 & 1 \\ -1 & -2 \end{bmatrix}$, $\boldsymbol{B}_p = \begin{bmatrix} 0 \\ 1 \end{bmatrix}$, $\boldsymbol{B}_\omega = \begin{bmatrix} 0.2 \\ 0.1 \end{bmatrix}$, $\boldsymbol{C}_p = [1 \quad 0]$, $\boldsymbol{D}_p = 0.5$ and the given gain matrix $\boldsymbol{K} = [-1 \quad 1 \quad 1]$. Here the reference model Eq. (24) is considered. Assuming $\tau_2 = 430$ ms, the minimum guaranteed $H\infty$ output tracking performances $\gamma$ for various values of $\tau_1$ are listed in Table 3. From Table 3, it can be seen that the obtained results are much better than the ones in Refs[17,19].

Table 3 Minimum value of $\gamma$ for $\tau_2 = 430$ ms

| Method\ $\tau_1$ | 0 | 50 ms | 100 ms | 150 ms | 200 ms |
|---|---|---|---|---|---|
| Ref. [17] | 3.9018 | 3.1017 | 2.5700 | 2.1922 | 1.91 |
| Ref. [19] | 1.6283 | 1.5795 | 1.5296 | 1.4783 | 1.4783 |
| Theorem 2 | 0.6402 | 0.8806 | 0.9595 | 0.9913 | 0.9798 |

In addition, the following system model in Refs[21,22] is considered.

$$\begin{cases} \dot{\boldsymbol{x}}_p(t) = \begin{bmatrix} 0 & 1 \\ -2 & -3 \end{bmatrix} \boldsymbol{x}_p(t) + \begin{bmatrix} 1 \\ 2 \end{bmatrix} \boldsymbol{u}(t) + \begin{bmatrix} 0.5 \\ 1 \end{bmatrix} \boldsymbol{\omega}(t) \\ \boldsymbol{y}_p(t) = [1 \quad 0] \boldsymbol{x}(t) \end{cases}$$

And the reference model is given by

$$\begin{cases} \dot{\boldsymbol{x}}_r(t) = -\boldsymbol{x}_r(t) + \boldsymbol{r}(t) \\ \boldsymbol{y}_r(t) = \boldsymbol{x}_r(t) \end{cases}$$

Assuming $\tau(t) \in [0, \quad 1.5\text{ ms})$, it is the same delay interval as Refs[21,22]. The obtained minimum guaranteed $H\infty$ output tracking performance $\gamma = 0.08$

by applying Theorem 2 is an important improvement over $\gamma = 3.012$ and $\gamma = 3.74$ obviously from Refs[21, 22], respectively.

**Example 3** In this example, the actual satellite system borrowing from Refs[17,19,31] is considered. The system consists of two rigid bodies joined together by a flexible link. Its state-space model is represented as

$$\begin{cases} \begin{bmatrix} \dot{\theta}_1(t) \\ \dot{\theta}_2(t) \\ \ddot{\theta}_1(t) \\ \ddot{\theta}_2(t) \end{bmatrix} = \begin{bmatrix} 0 & 0 & 1 & 0 \\ 0 & 0 & 0 & 1 \\ -0.09 & 0.09 & -0.04 & 0.04 \\ 0.09 & -0.09 & 0.04 & -0.04 \end{bmatrix} \begin{bmatrix} \theta_1(t) \\ \theta_2(t) \\ \dot{\theta}_1(t) \\ \dot{\theta}_2(t) \end{bmatrix} + \begin{bmatrix} 0 \\ 0 \\ 1 \\ 0 \end{bmatrix} \boldsymbol{u}(t) + \begin{bmatrix} 0 \\ 0 \\ 0 \\ 1 \end{bmatrix} \boldsymbol{\omega}(t) \\ \boldsymbol{y}(t) = [0 \quad 1 \quad 0 \quad 0] [\theta_1^T \quad \theta_2^T \quad \dot{\theta}_1^T \quad \dot{\theta}_2^T]^{\mathrm{T}} \end{cases}$$

here reference model Eq. (24) is still considered. The minimum guaranteed $H\infty$ output tracking perfor-mances $\gamma$ for different delay intervals $\tau(t)$ are listed in Table 4.

The sampling period $h = 15$ ms is set. $\tau_1 = 5$ ms and $\tau_2 = 30$ ms are chosen as the same to Refs[17, 19]. By solving the inequalities presented in Theorem 2, the minimum guaranteed $H\infty$ output tracking performance $\gamma = 0.0721$ is obtained with the controller gain $\boldsymbol{K} = [-110 \quad -221430 \quad -50 \quad -24520 \quad 99080]$. From Table 4, it can be seen the obtained result is considerably less conservative than the previous results. And the improvement over the result from Ref. [19] ($\gamma = 0.0915$) is as high as 27%.

Table 4 Minimum value of $\gamma$ for different delay interval

| Method\ $\tau(t)$ | $\tau(t) \in [5\text{ms}, 30\text{ms})$ | $\tau(t) \in [5\text{ms}, 20\text{ms})$ |
|---|---|---|
| Ref. [17] | 0.1267 | / |
| Ref. [19] | 0.0915 | / |
| Ref. [31] | / | 0.07 |
| Theorem 2 | 0.0721 | 0.0520 |

The system's output obtained from Theorem 2 and Ref. [19], and the reference's output are shown in Fig. 4. It is clear that the proposed method provides better result. The tracking error obtained by using Theorem 2 is compared with the results from the controller proposed in Ref. [19], and the result is shown in Fig. 5. It can be seen that the output tracking error is also further reduced by the proposed method in this paper.

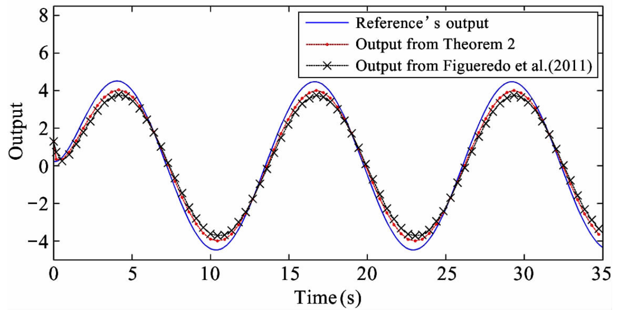


**Fig. 4** Reference's output $\boldsymbol{y}_r(t)$, system's output $\boldsymbol{y}(t)$ from Theorem 2 and from Figueredo et al. (2011) in Ref. [19] (Example 3)

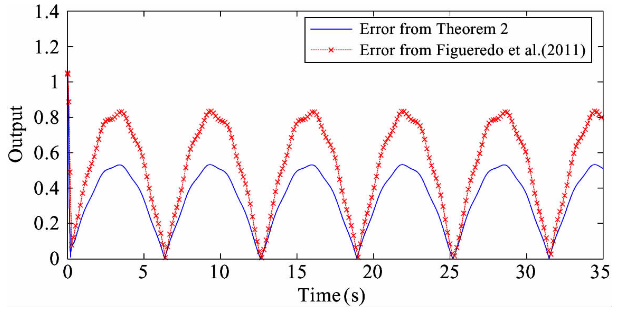


**Fig. 5** Output tracking error from Theorem 2 compared with the results from Figueredo et al. (2011) in Ref. [19] (Example 3)

## 5 Conclusions

A novel method for the $H\infty$ output tracking analysis and control design for NCSs with consideration of network-induced delays, packet dropouts, parameter uncertainties and external disturbance is proposed. By considering the piecewise differentiable characteristic of the time delay and using the new approach of free weighting matrix, reciprocally convex and CCL, the better $H\infty$ output tracking performance is obtained. Moreover, the proposed method is also suitable for the NCSs stability problem and yields less conservative results. In the end, the results of numerical examples show the effectiveness of the proposed $H\infty$ output tracking control design, and illustrate the advantages of our criteria which outperform previous criteria in the literature.

### References

[1] Hespanha J P, Naghshtabrizi P, Xu Y. A survey of recent results in networked control systems[J]. *Proceedings of the IEEE*, 2007, 95(1): 138-162
[2] Gupta R A, Chow M Y. Networked control system: overview and research trends[J]. *IEEE Transactions on Industrial Electronics*, 2010, 57(7): 2527-2535
[3] Zhang D, Shi P, Wang Q G, Yu L. Analysis and synthesis of networked control systems: a survey of recent advances and challenges[J]. *ISA Transactions*, 2016, 66: 376-392

[ 4] Tan C, Li L, Zhang H S. Stabilization of networked control systems with both network-induced delay and packet dropout[J]. *Automatica*, 2015, 59: 194-199
[ 5] Bauer N W, Maas P J H, Heemels W P M H. Stability analysis of networked control systems: a sum of squares approach[J]. *Automatica*, 2012, 48(8): 1514-1524
[ 6] Qiu L, Luo Q, Gong F, et al. Stability and stabilization of networked control systems with random time delays and packet dropouts[J]. *Journal of the Franklin Institute*, 2013, 350(7): 1886-1907
[ 7] Elahi A, Alfi A. Finite-time $H\infty$ control of uncertain networked control systems with randomly varying communication delays[J]. *ISA Transactions*, 2017, 69: 65-88
[ 8] Liu Y Z, Li M G. An improved delay-dependent stability criterion of networked control systems[J]. *Journal of the Franklin Institute*, 2014, 351(3): 1540-1552
[ 9] Jayawardhana B, Weiss G. Tracking and disturbance rejection for fully actuated mechanical systems[J]. *Automatica*, 2008, 44(11):2863-2868
[10] Pan H H, Sun W C, Jing X J. Adaptive tracking control for stochastic mechanical systems with actuator nonlinearities[J]. *Journal of the Franklin Institute*, 2017, 354(7): 2725-2741
[11] Huang J S, Wen C Y, Wang W, et al. Adaptive output feedback tracking control of a nonholonomic mobile robot [J]. *Automatica*, 2014, 50(3): 821-831
[12] Liao F, Wang J L, Yang G H. Reliable robust flight tracking control: an LMI approach[J]. *IEEE Transactions on Control Systems Technology*, 2002,10(1): 76-89
[13] Pang Z H, Liu G P, Zhou D, et al. Output tracking control for networked systems: a model-based prediction approach[J]. *IEEE Transactions on Industrial Electronics*, 2014, 61(9):4867-4877
[14] Zhang J H, Lin Y J, Shi P. Output tracking control of networked control systems via delay compensation controllers[J]. *Automatica*, 2015, 57: 85-92
[15] Lu R, Xu Y, Zhang R. A new design of model predictive tracking control for networked control system under random packet loss and uncertainties[J]. *IEEE Transactions on Industrial Electronics*, 2016, 63(11):6999-7007
[16] Zhang H, Shi Y, Xu M, et al. Observer-based tracking controller design for networked predictive control systems with uncertain Markov delays[J]. *International Journal of Control*, 2013, 86(10):1824-1836
[17] Gao H J, Chen T W. Network-based H∞ output tracking control[J]. *IEEE Transactions on Automatic Control*, 2008, 53(3): 655-667
[18] Wouw N V D, Naghshtabrizi P, Cloosterman M B G, et al. Tracking control for sampled-data systems with uncertain time-varying sampling intervals and delays[J]. *International Journal of Robust & Nonlinear Control*, 2010, 20(4): 387-411
[19] Figueredo L F C, Ishihara J Y, Borges G A, et al. Delay-dependent robust $H\infty$ output tracking control for uncertain networked control systems[C]. In: Proceedings of the 18th IFAC World Congress, Milan, Italy, 2011. 3256-3261
[20] Zhang D W, Han Q L, Jia X C. Observer-based H∞ output tracking control for networked control systems[J]. *International Journal of Robust and Nonlinear Control*, 2013, 24(17): 2741-2760
[21] Wu Y, Wu Y P. $H\infty$ output tracking control over networked control systems with Markovian jumping parameters[J]. *Optimal Control Applications & Methods*, 2016, 37(6): 1162-1174
[22] Wu Y, Liu T S, Wu Y P, et al. $H\infty$ output tracking control for uncertain networked control systems via a switched system approach[J]. *International Journal of Robust & Nonlinear Control*, 2016, 26(5): 995-1009
[23] Wu M, He Y, She J H, et al. Delay-dependent criteria for robust stability of time-varying delay systems[J]. *Automatica*, 2004, 40(8): 1435-1439
[24] Zeng B H, He Y, Wu M, et al. Free-matrix-based integral inequality for stability analysis of systems with time-varying delay[J]. *IEEE Transactions on Automatic Control*, 2015, 60(10): 2768-2772
[25] Seuret A, Gouaisbaut F. Wirtinger-based integral inequality: application to time-delay systems[J]. *Automatica*, 2013, 49(9): 2860-2866
[26] Zhang C K, He Y, Jiang L, et al. Stability analysis of systems with time-varying delay via relaxed integral inequalities[J]. *Systems & Control Letters*, 2016, 92: 52-61
[27] Park P G, Ko J W, Jeong C. Reciprocally convex approach to stability of systems with time-varying delays [J]. *Automatica*, 2011, 47(1): 235-238
[28] Zhang C K, He Y, Jiang L, et al. An extended reciprocally convex matrix inequality for stability analysis of systems with time-varying delay[J]. *Automatica*, 2017, 85: 481-485
[29] Zhang X M, Han Q L. A delay decomposition approach to delay-dependent stability for linear systems with time-varying delays[J]. *International Journal of Robust & Nonlinear Control*, 2009, 19(17): 1922-1930
[30] Zeng H B, He Y, Wu M, et al. Less conservative results on stability for linear systems with a time-varying delay [J]. *Optimal Control Applications & Methods*, 2013, 34(6): 670-679
[31] Peng C, Song Y, Xie X P, et al. Event-triggered output tracking control for wireless networked control systems with communication delays and data dropouts[J]. *IET Control Theory & Applications*, 2016, 10(17): 2195-2203
[32] Han Q L. Absolute stability of time-delay systems with sector-bounded nonlinearity[J]. *Automatica*, 2005, 4: 2171-2176
[33] Tian E G, Yue D, Zhang Y J. Delay-dependent robust H∞ control for T-S fuzzy system with interval time-varying delay[J]. *Fuzzy Sets and Systems*, 2009, 160(12): 1708-1719
[34] Wang C, Shen Y. Delay-dependent non-fragile robust stabilization and H∞ control of uncertain stochastic systems with time-varying delay and nonlinearity[J]. *Journal of the Franklin Institute*, 2011, 348(8): 2174-2190
[35] He Y, Wu M, Liu G P, et al. Output feedback stabilization for a discrete-time system with a time-varying delay [J]. *IEEE Transactions on Automatic Control*, 2008, 53(10): 2372-2377

**Liu Yicai**, born in 1982. He is currently pursuing the Ph. D. degree in control theory and control engineering at Wuhan University of Science and Technology, Wuhan, China. He received the B. S. degree in communication engineering from China University of Geosciences, Wuhan, China, in 2005, and the M. S. degree from Institute of Modern Physics, Chinese Academy of Sciences, Lanzhou, China, in 2008. His research focuses on networked control systems and predictive control.